

Gross Theory Model for Neutrino-Nucleus Cross Section

A. R. Samana^{1,2,†}, C. A. Barbero^{3,4,*}, S. B. Duarte²,
A. J. Dimarco⁵ and F. Krmpotić^{6,7}

¹Department of Physics Texas A&M University-Commerce, P.O.Box 3011 ,
Commerce, Texas, USA

²Centro Brasileiro de Pesquisas Físicas, Rua Dr. Xavier Sigaud 150, CEP 22290-180,
Rio de Janeiro-RJ, Brazil

³Instituto de Física La Plata, CONICET, 1900 La Plata, Argentina

⁴Departamento de Física, Facultad de Ciencias Exactas, Universidad Nacional de La
Plata, C.C. 67, 1900 La Plata, Argentina

⁵Departamento de Ciências Exactas e Tecnológicas, Universidade Estadual de Santa
Cruz, CEP 45662-000 Ilhéus, Bahia-BA, Brazil

⁶Departamento de Física Matemática, Instituto de Física da Universidade de São
Paulo, Caixa Postal 66318, 05315-970 São Paulo-SP, Brazil

⁷Facultad de Ciencias Astronómicas y Geofísicas, Universidad Nacional de La Plata,
1900 La Plata, Argentina.

E-mail: † arturo@cbpf.br

* barbero@fisica.unlp.edu.ar

Abstract. The nuclear gross theory, originally formulated by Takahashi and Yamada for the β -decays, is applied for the electronic-neutrino nucleus reactions, employing a more realistic description to the energetics of the Gamow-Teller resonances. The model parameters are gauged from the most recent experimental data, both for β^- decay and electron-capture, separately for even-even, even-odd, odd-odd, odd-even nuclei. The numerical estimates for neutrino-nucleus cross sections agree fairly well with previous evaluations done within the framework of microscopic models. The formalism presented here can be extended to the heavy nuclei mass region, where weak processes are quite relevant, which is of astrophysical interest because of its applications in supernova explosive nucleosynthesis.

PACS numbers: 21.60.-n, 21.10.-k

1. Introduction

The nucleosynthesis of heavy elements is only understood if stellar reactions take place in regions of nuclear chart far away from the β -stability line, involving a large number of unstable or even exotic nuclear species for which the experimental data are very scarce. For instance, the steps of nucleosynthesis in the r -process occurs out to and just along the neutron drip line where many of principal nuclear properties are still unknown. Great theoretical and experimental efforts have been invested in the last decades in order to describe the nuclear properties of different species along the β -stability line, as well as those of exotic nuclei involved in explosive nucleosynthesis processes [1, 2, 3].

The theoretical models can be separated generically into: i) the macroscopic models which describe the global nuclear properties [4, 5, 6, 7, 8, 9, 10], and where special attention is paid to the *gross theory of the β -decay* (GTBD); and ii) the microscopic formalisms *i.e.*, the shell model or RPA based calculations [10, 11, 12, 13] where detailed nuclear structure of each species is considered.

The GTBD was first proposed by Takahashi and Yamada [4] nearly forty years ago to describe the global properties of allowed β -decay processes. It is essentially a parametric model, which attempted to combine the single-particle and statistical arguments in a phenomenological way. Afterwards, different versions of the 'gross theory' have been developed and used for practical applications very frequently [5, 6, 7, 8, 9]. This is due to: i) their simplicity when compared with the hard computational work involved in the implementation of the microscopic models, and ii) their capability to reproduce the available experimental data, and to be extrapolated later on to unknown nuclei far away from the β -stability line. In fact, as these theoretical approaches account systematically and fairly well for the properties of stable nuclei, they have been extensively applied to describe: 1) the β -decay half-lives and other nuclear observables participating in the r -process, and 2) the properties of a great number of exotic nuclei that are involved in the nucleosynthesis.

It also should be mentioned that the gross-theory approach has been also used by N. Itoh *et al.*, in Refs. [14] for the calculation of the total capture of a neutrino by ^{37}Cl , ^{16}O , ^{20}Ne and ^{56}Fe nuclei, which are used in the detection of solar neutrinos.

The aim of the present work is twofold. First, motivated by the simplicity of the original GTBD, we use it to evaluate the half-lives of allowed weak-transitions (β -decay and electron-capture) in nuclei with $A < 70$, which are of major importance for the presupernova collapse processes. We also analyze the consequences of employing a more realistic estimate for the energetic of the Gamow-Teller resonance (GTR) than in the previous works. This will lead us to a new trend for the adjustable parameter related to the energy spread of the GTR caused by the spin dependent part of the nuclear force. Second, we use the same gross-theory approach to describe the nuclear neutrino capture over a great number of nuclei involved in presupernova structure with the purpose to extend in the future the calculation to r -process in neutrino rich environment. Since within the stellar conditions no experimental data exist, our results are confronted with

those achieved in the framework of microscopic approaches.

The paper is organized as follows. In Sect. 2 we briefly sketch the conventional gross-theory for nuclear β -decay and electron capture rate. In Sect. 3 we introduce the gross theory for the evaluation of the neutrino-nucleus reaction cross-section. The single-particle strength functions are discussed in Sects. 4 and 5, together with the estimate of the GTR energy and the procedure used to derive the corresponding spread of the transition strength. In Sect. 6 we exhibit and discuss our results. Summarizing conclusions and future extension of the present work are drawn in Sect. 7.

2. Gross theory of nuclear beta decay (GTBD)

The GTBD permits to evaluate the half-lives of β^\pm -decay and the rates for electron capture weak processes. As an example, we briefly sketch here the original GTBD [4] for the decay $(Z, A) \rightarrow (Z + 1, A) + e^- + \tilde{\nu}$. The total rate for allowed transitions is written (in natural units) as

$$\lambda_\beta = \frac{G_F^2}{2\pi^3} \int_{-Q_\beta}^0 dE \left[g_V^2 |\mathcal{M}_F(E)|^2 + g_A^2 |\mathcal{M}_{GT}(E)|^2 \right] f(-E), \quad (1)$$

where $G = (3.034545 \pm 0.00006) \times 10^{-12}$ is the Fermi weak coupling constant, $g_V = 1$ and $g_A = -1$ are, respectively, the vector and axial-vector coupling constants ‡. The argument of the matrix element (E) is the transition energy measured from the parent ground state. Note that the true β -decay transition energy is $E_\beta = E_e + E_\nu = -E > 0$. The usual integrated dimensionless Fermi function [15, 16], $f(E)$, is evaluated from the approximated formulas given in Ref.[4] that are correct up to $\sim 10\%$ for standard decays. The Q_β -value is the difference between neutral atomic masses of parent and daughter nuclei:

$$Q_{\beta^-} = M(A, Z) - M(A, Z + 1) = B(A, Z + 1) - B(A, Z) + m(nH) \quad (2)$$

with $B(A, Z)$ and $B(A, Z + 1)$ being the corresponding nuclear binding energies, and $m(nH) = m_n - m(^1H) = m_n - m_p - m_e = 0.782$ MeV. The masses were obtained in the same way as in Ref. [7]. This means that, when available, they are taken from Wapstra-Audi-Hoekstra mass table [17] and, otherwise, they are determined from Tachibana-Uno-Yamada semi-empirical mass formula [18].

The squares of the Fermi (F) and Gamow-Teller (GT) matrix elements are determined as:

$$|\mathcal{M}_X(E)|^2 = \int_{\epsilon_{min}}^{\epsilon_{max}} D_X(E, \epsilon) W(E, \epsilon) \frac{dn_1}{d\epsilon} d\epsilon, \quad \text{for } X = F, GT. \quad (3)$$

Here, ϵ_{min} is the lowest single-particle energy of the parent nucleus and ϵ_{max} is the energy of the highest occupied state. The one-particle level density (proton or neutron), $dn_1/d\epsilon$, is determined by Fermi gas model for the parent nucleus, and the weight function

‡ Finite nuclear size effects are incorporated via the dipole form factor $g \rightarrow g \left(\frac{\Lambda^2}{\Lambda^2 + k^2} \right)$ where k is the momentum transfer and $\Lambda = 850$ MeV the cutoff energy.

$W(E, \epsilon)$, constrained by $0 \leq W(E, \epsilon) \leq 1$, takes into account the Pauli blocking. Finally, $D_x(E, \epsilon)$, normalized as $\int_{-\infty}^{+\infty} D_x(E, \epsilon) dE = 1$, is the probability that a nucleon with single-particle energy ϵ makes a β -transition. As in Ref. [4] we neglect the ϵ -dependence, *i.e.*, it is assumed that all nucleons have the same decay probability, independently of their energies ϵ , $D_x(E, \epsilon) \equiv D_x(E)$. The GTBD characterizes this $D_x(E)$ through their energy weight moments (for example, in [14] these expressions were written explicitly).

The dependence on the odd-even proton and neutron numbers in the daughter nucleus is introduced through the values for the pairing gap Δ and the single-particle level spacing d . In the present work we adopted those from Ref. [5]. More details on the probability function $D_x(E)$ are given in Sect. 4.

The original GTBD [4] has been gradually improved [6, 7], and nowadays we have two new versions: the first is named the 2nd generation gross theory (GT2), and the second is the so called semi-gross theory (SGT) in which some parts of nuclear shell effects are considered. The most recent GT2 and SGT approaches use an updated mass formula, and they better account for the shell and pairing effects [7, 9].

3. Gross theory of nuclear neutrino capture (GTNC)

In the most recent versions of r -processes nucleosynthesis in supernova, one considers that these processes take place on the surface of a proton-neutron star during the supernova collapse. The nuclei are exposed there to a thermal flux $\Phi_\nu(E_\nu)$ of ν_e with energy E_ν , which causes the reaction $\nu_e + (Z, A) \rightarrow (Z + 1, A) + e^-$, with cross-section [12, 10, 19]

$$\langle \sigma_\nu \rangle = \int_{E_{th}}^{\infty} \Phi_\nu(E_\nu) \sigma_\nu(E_\nu) dE_\nu, \quad (4)$$

where E_{th} is the reaction energy threshold, which is equal to the Q_β -value for stable nuclei and zero for unstable cases. For $\Phi_\nu(E_\nu)$ we take a zero-chemical potential Fermi-Dirac distribution

$$\Phi_\nu(E_\nu) = \frac{\mathcal{N}}{T_\nu^3} \frac{E_\nu^2}{e^{E_\nu/T_\nu} + 1}, \quad (5)$$

where T_ν is the neutrino temperature, and \mathcal{N} is the normalization constant of the spectrum [12].

The evaluation of the ν_e -nucleus cross-section $\sigma_\nu(E_\nu)$, in a neutrino-rich environment, must be consistent with the procedure employed in calculating the β -decay rates. The allowed transition approximation (see [19, Eq.(2.19)])

$$\sigma_\nu(E_\nu) = \frac{G^2}{\pi} \int_0^{E_\nu - m_e} p_e E_e F(Z + 1, E_e) \left[g_V^2 |\mathcal{M}_F(E)|^2 + g_A^2 |\mathcal{M}_{GT}(E)|^2 \right] dE, \quad (6)$$

can be applied for relatively small momentum transfer. The integration covers all possible nuclear states allowed by the selection rules, and the integration limits are determined from the energy conservation condition. When the energies are measured from the ground state of the parent nucleus (Z, A) , this condition reads

$$E_\nu + M(Z, A) = E_e + M(Z + 1, A) + Q_{\beta^-} + E, \quad (7)$$

where $E = E_\nu - E_e > 0$ is the excitation energy of daughter nucleus $(Z + 1, A)$, and $F(Z, E)$ is the usual scattering Fermi function which takes into account the Coulomb interaction between the electron and the nucleus.

4. Single-particle strength functions

A key element in the gross theory is the single-particle strength probability function $D_x(E)$. The successive improvements of the theory have used gaussian-, exponential-, and lorentzian-type functions [4, 7]. The sec-hyperbolic functions have been employed in the GT2 [7]. Here we will mainly adopt the gaussian-like behavior for the transition strengths. To illustrate that the calculations are rather independent of the functional form adopted for $D_x(E)$, a comparison will be done between the results obtained with the gaussian-like distribution

$$D_x(E) = \frac{1}{\sqrt{2\pi}\sigma_x} e^{-(E-E_x)^2/(2\sigma_x^2)}, \quad (8)$$

and those calculated with the lorentzian-type strength function

$$D_x(E) = \frac{\Gamma_x}{2\pi} \frac{1}{(E - E_x)^2 + (\Gamma_x/2)^2}. \quad (9)$$

Here E_x is the resonance energy, σ_x is the standard deviation, and the other quantities are defined as in Ref. [4].

When isospin is a good quantum number the total Fermi strength $\int |\mathcal{M}_F(E)| dE = N - Z$ is carried entirely by the isobaric analog state (IAS) in the daughter nucleus. However, because of the Coulomb force, the isospin is not a good quantum number and this leads to the energy splitting of the Fermi resonance. We will use the estimates introduced by Takahashi and Yamada [4], namely

$$\begin{aligned} E_F &= \pm (1.44ZA^{-1/3} - 0.7825) \text{ MeV}; & \text{for } \beta^\pm \text{ decay,} \\ \sigma_F &= 0.157ZA^{-1/3} \text{ MeV.} \end{aligned} \quad (10)$$

The total GT strength in the (ν_e, e^-) channel is given by the Ikeda sum rule $\int |\mathcal{M}_{GT}(E)| dE \cong 3(N - Z)$, but its distribution cannot be established by general arguments, and therefore must be either calculated or measured. Charge-exchange reactions (p, n) have demonstrated that most of the strength is accumulated in a broad resonance near the IAS [20]. In fact, even before these measurements have been performed, Takahashi and Yamada [4] have used the approximation

$$E_{GT} \cong E_F, \quad (11)$$

while σ_{GT} is expressed as

$$\sigma_{GT} = \sqrt{\sigma_F^2 + \sigma_N^2}, \quad (12)$$

with σ_N being the energy spread caused by the spin dependent nuclear forces.

For the Fermi transitions we use the relation (10). Yet, for the GT resonance, instead of employing the approximation (11), we use the estimate

$$E_{GT} = E_F + \delta; \quad \delta = 26A^{-1/3} - 18.5(N - Z)/A \quad \text{MeV}, \quad (13)$$

obtained by Nakayama *et al.* [21] from the analytic fit of the (p, n) reaction data of nuclei near stability line [20], where δ is positive. For the standard deviation σ_{GT} we preserve the expression (12), and σ_N is treated as an adjustable parameter. Note that the two terms of δ in (13) have well defined physical interpretations. The first one is due to the $SU(4)$ symmetry breaking imposed by the spin-orbit coupling, and it is of the same order of magnitude as the Bohr-Mottelson estimate for the spin-orbit splitting ($\Delta_{ls} \cong 20A^{-1/3}$ MeV), obtained from the approximation $l \cong A^{1/3}$ [22]. The second term is responsible for the partial restoration of the $SU(4)$ symmetry, having the same mass and charge dependence as the difference between the energy shifts produced by the GT and Fermi residual interactions. We remark that the Eq. (13) is frequently used in the study of r -process in neutron rich nuclei [10, 23, 24, 25, 26, 27, 28, 29, 30, 31, 32]. There $\delta < 0$, and therefore the GTR falls below the IAS, as happens in the shell-model calculation [10]. \mathcal{S}

5. Fitting Procedure

Another important aspect in implementing the GTBD is the choice of the χ^2 -minimization method that is used to derive the width parameter σ_N . In the original work of Takahashi and Yamada [4] is minimized the quantity

$$\chi_A^2 = \sum_{n=1}^{N_0} \left[\log \left(\tau_{1/2}^{cal}(n) / \tau_{1/2}^{exp}(n) \right) \right]^2, \quad (14)$$

where N_0 is the number of experimental β -decay half-lives, $\tau_{1/2}^{exp}$, fulfilling the conditions: 1) the branching ratio of the allowed transitions exceeds $\sim 50\%$ of the total β -decay branching ratio, and 2) the ground state Q -value is $\geq 10A^{-1/3}$ MeV.

In the present work σ_N is determined through the minimization of the function

$$\chi_B^2 = \sum_{n=1}^{N_0} \left[\frac{\log(\tau_{1/2}^{cal}(n) / \tau_{1/2}^{exp}(n))}{\Delta \log(\tau_{1/2}^{exp}(n))} \right]^2, \quad (15)$$

where

$$\Delta \log(\tau_{1/2}^{exp}(n)) \equiv \left| \log[\tau_{1/2}^{exp}(n) + \delta\tau_{1/2}^{exp}(n)] - \log[\tau_{1/2}^{exp}(n)] \right|, \quad (16)$$

and $\delta\tau_{1/2}^{exp}$ is the experimental error. Thus, the χ_B^2 -function reinforces the contributions of data with small experimental errors. Moreover, we perform different fittings for even-even, odd-odd, odd-even and even-odd nuclei. Needless to say that for $\tau_{1/2}^{exp}$ we use here the most recent data [33], instead of those that were available when the GTBD has been formulated [4]. The condition $\log ft \leq 6$ is imposed to include only the allowed β -decays.

\mathcal{S} Occasionally is used the fit [7]

$$E_{GT} = E_F + \delta'; \quad \delta' = 6.7 - 30(N - Z)/A \quad \text{MeV},$$

which also reproduces satisfactorily the stable nuclei. The second term of δ' is interpreted in the same way as that of δ in (13), but the first term here does not have any direct physical significance.

6. Numerical results and discussion

6.1. β^- decay and electron-capture half-lives

For the single-particle strength probability function $D_X(E)$ we adopt the gaussian-like behavior (8) in most of the calculations. The corresponding values of the adjustable parameters at the minimal value of the χ^2 -function, χ_{min}^2 , are listed in Table I for the four different parity families of nuclei. They are labeled as σ_N^* and σ_N , when for E_{GT} are used, respectively, the Eqs. (11) and (13). One sees that σ_N is always larger than σ_N^* , which means that the effect of using more realistic energies E_{GT} is reflected in the increase of the standard deviations. The values of σ_N^* derived in Ref. [4] are exhibited parenthetically in Table I. It is important to point out that the difference between the old and new values for σ_N^* does not comes from the fitting procedure itself, but from the different samples of nuclei employed here for each parity family.

Figure 1 shows the dependence of χ^2/χ_{min}^2 on both: i) the energy of the GTR (left panels for (11), and right panels for (13)), and ii) the type of the minimization function (upper panels for (14), and lower panels for (15)). We note that the χ_B^2 -functions present rather pronounced minima when compared with those of the χ_A^2 -functions. More, in most of the cases the χ_B^2 minima are located at smaller values of the standard deviations than the χ_A^2 ones. This is a direct consequence of including the experimental errors in the minimization procedure of the χ_B^2 -function.

In order to estimate the average deviation of our results, we have computed the mismatch factor η defined as [4]

$$\eta = 10\sqrt{\chi^2/N_0} \quad , \quad (17)$$

showing their values for each σ_N in Table 1, and similarly the values of η^* corresponding to each σ_N^* . It can be observed that the χ_B^2 minimization procedure considerably reduces the mismatch factor, in particular for odd-odd family of nuclei. Thus, we can say that the use of χ_B^2 -function modifies σ_N and leads to a better statistical agreement between the theoretical results and the experimental data.

Figure 2 compares the experimental β^- -decay half-lives within the Mn isotopic chain with our results obtained for the σ_N values from Table 1. One can see that the GTBD overestimates the data. However, it should be pointed out that this disagreement is not characteristic of the GTBD, since other microscopic and global models lead to similar results. For instance, this is the case of: a) the extended Thomas-Fermi plus Strutinsky integral method combined with the continuum quasiparticle random phase approximation (ETFSI+CQRPA) [12], and b) the extended Thomas Fermi method combined with the semi-gross theory (ETFSI+GT2) [7].

Figure 3 shows the distribution of $\log(\tau_{1/2}^{cal}/\tau_{1/2}^{exp})$, as a function of $Q_\beta A^{-1/3}$, for β^- -decay. We observe that the results obtained with Eqs. (11) and (13) are quite similar to each other for same parity families, the first one being somewhat larger. We can also see that for the odd-odd family a very good agreement between theoretical and experimental results is obtained for $Q_\beta A^{1/3} \geq 45$ MeV, while for the other three families this happens

already for $Q_\beta A^{1/3} \geq 40$ MeV. Thus, as frequently mentioned in the literature [4, 7, 9], the best GTBD results are obtained for heavy nuclei.

In the evaluation of the allowed electron-capture and β^+ -decay rates for nuclei of $A < 70$ we have re-adjusted the parameter σ_N , imposing again the constraint $\log ft < 6$. The resulting values of σ_N and η for the two χ^2 -function, with E_{GT} calculated from Eq. (13), are presented in Table 2. Figure 4 shows the values of $\log(\tau_{1/2}^{calc}/\tau_{1/2}^{exp})$ as a function of $Q_\beta A^{1/3}$ for the electron-capture rates calculated with the underlined σ_N values listed in Table 2. Similar general features to those remarked in the β^- -decay case are obtained.

Also, we briefly discuss the dependence of the χ^2 procedure on the functional form of the employed strength distribution. Thus, we repeat the calculations for β^- -decay and electron-capture rates using now the lorentzian distribution D_X , given by the Eq. (9), together with the Eq. (13) for the GT energy. The resulting Γ_N energies are shown in Table 3, and the corresponding $\log(\tau_{1/2}^{calc}/\tau_{1/2}^{exp})$ values for the β^- emitter nuclei with $A < 70$ exhibit similar $Q_\beta A^{1/3}$ dependence to that shown in Figure 3.

Figure 5 shows the results for the electron-capture rates along the Ni isotopic chain. The calculations with the gaussian and lorentzian strength functions turn out to be quite similar to each other and both show a reasonable agreement with the data.

6.2. Neutrino-nucleus cross section

The reduced thermal cross section $\langle\sigma_\nu\rangle/A$ of the four β^- emitter families was evaluated for the $A < 70$ nuclei with two sets of parameters, σ_N^* and σ_N . The results, confronted in Figure 6, indicate that the Eq. (13) always yields smaller values for this quantity than those obtained with the Eq. (11), the difference being more pronounced for $A > 30$. However, for some isolated light nuclei, the use of a more realistic GTR energy increases the cross section. This is the case of ^{12}B , for which the product $\sigma(E_\nu)\Phi(E_\nu)$ is shown in the left panel of Figure 7. The increase of $\sigma(E_\nu)$ arises from the contribution of the 1^+ states with energies below the GTR (see Refs. [19, 34]). As another example, in the right panel of Figure 7 are shown the results for the Ni isotopes (^{67}Ni , ^{68}Ni and ^{69}Ni). One notes that for the three nuclei, the product $\sigma(E_\nu)\Phi(E_\nu)$ decreases when the energy of the GTR is moved up. Also, because of the pairing effect, the cross-section in ^{68}Ni presents the lowest value for both GT energies.

On the other hand, from Figure 8 it can be seen that our results for the reduced thermal cross-section in Ni nuclei emphasizes the odd-even effect when compared with the microscopic ETFSI+CQRPA calculation [12], where this effect seems to be washed out. This leads a different trend of the ν_e -nucleus cross section with respect to A .

For completeness, in Figure 9 we present the results for $\langle\sigma_\nu\rangle/A$ obtained with the GTNC, both for the β^- -decaying nuclei (with σ_N from Table 1), and for the nuclei where take place electron-capture (with σ_N from Table 2).

It is worth noticing that the gaussian and lorentzian strength functions given, respectively, by Eqs. (8) and (9) yield almost the same results for the reduced thermal

cross-sections.

At this point it is important to clarify the meaning of the thermal neutrino flux presented in Eq. (5), which we have used for the calculation of the thermal neutrino-nucleus cross section $\langle\sigma_\nu\rangle$. This neutrino energy flux is given by a Fermi distribution, *i.e.*, Eq. (5) depending explicitly on the temperature parameter T_ν . In order to compare our results with those of Borzov and Goriely [12] we have used here a constant temperature $T_\nu = 4$ MeV. However, this situation could not be a realistic one for the supernova neutrino wind. Neutrinos (and antineutrinos) with different energies and flavors decouple at different points of the supernova core and the neutrino spectrum, in fact could be non thermal. This is due to the non-thermalization of neutrinos through their transport along hydrodynamics medium evolution [35, 36]. Thus, it could be interesting to determine the consequences of employing a different neutrino flux such as a power law flux of the form

$$\Phi_\nu(E_\nu) = \mathcal{N}_{PL} \left(\frac{\epsilon_\nu}{\langle\epsilon_\nu\rangle} \right)^\alpha e^{-\frac{(\alpha+1)\epsilon_\nu}{\langle\epsilon_\nu\rangle}}. \quad (18)$$

The parameters $\langle\epsilon_\nu\rangle$ and α are not fully determined and here we take $\langle\epsilon_\nu\rangle \approx 3.1514 T_\nu = 12.6056$ MeV, and $\alpha \approx 2.3014$, which reproduces better the Fermi-Dirac neutrino distribution function in Eq. (5) using $T_\nu = 4$ MeV. These parameter values were obtained in Ref. [35]. The normalization constant \mathcal{N}_{PL} ensures unitary flux between 0 and 102 MeV. We have found that, for all practical purposes, the flux (18) yields the same results as the thermal flux (5). This is an expected result, since these two fluxes tend to behave differently only in the tail zone, far away of the integration interval used to obtain the $\sigma_\nu(E)$ for astrophysical applications. Some possible deviations in the tail of these fluxes are important for the rate of nuclear reactions in studies of astrophysics plasmas [37].

7. Summarizing conclusions

We have briefly revived the original version of the gross theory for the β -decay. The main improvement introduced is a more realistic estimate for the location of the GTR energy peak, E_{GT} . After fixing the free parameter of our model (σ_N or Γ_N , depending on the parametrization adopted for the strength function) we have calculated the β^- -decay and electron-capture rates. A careful selection of input data for $A < 70$ nuclei, with small error bars in the measured half-lives, has been done in order to fix the model parameters in the fitting procedure. The model can be extended to the $A > 70$ nuclei, as well as to the transuranic nuclei, which are of interest for the study of the r -process in supernova. The first- and second-forbidden weak processes could play an important role in the exotic nuclei within this nuclear mass region. But, these transitions can be easily included in the gross theory framework, as has been done already by Nakata *et al.* [9] within the semi-gross theory ||.

|| A relation analogous to (13) was also derived for the first forbidden charge-exchange resonances [38], which is quite different to the one used in Ref. [9]. Thus it might be more appropriate to employ [38,

The present results are encouraging, in the sense that the gross theory could be able to describe in a systematic way, not only the nuclear properties along the β -stability line, but also for exotic nuclei involved in presupernova composition. In particular, the results for the reduced thermal cross section $\langle\sigma_\nu\rangle/A$ in the region $A < 70$ are in fair agreement with previous calculation performed within more refined microscopic models, *i.e.*, the EFTSI+CQRPA model [12]. The difference between the two descriptions could be attributed to the use of the Fermi gas model which contains more degrees of freedom than the EFTSI+CQRPA. Consequently, in general, $\sigma_\nu(E_\nu)$ calculated with the Fermi gas model leads to values higher than those obtained with microscopical nuclear models [39, 40, 41], particularly for light or intermediated nuclei (see, for instance, the results for the $\nu - {}^{12}\text{C}$ reaction shown in [9, Fig. 2]) and [41, Fig. 32]).

The important aspect of the recent r -process calculations is that they take into account the neutrino-rich environment in supernova explosion, where the ν_e -nucleus reaction are in competition with the β -decay processes [42]. To address this type of calculation we have evaluated the cross-section $\sigma_\nu(E_\nu)$ within the GTNC model, folded with a temperature dependent neutrino flux.

Finally, we want to remark once more the simplicity of the present model, which we are planing to extended in the near future to the r -process nuclei region, as well as to evaluate the isotopic abundances in presupernova scenario.

Acknowledgments

A.R.S. thanks the financial support of FAPERJ (Rio de Janeiro, Brasil) and from Texas A&M University-Commerce. Two of us (C.A.B. and F.K.) are members of CONICET (Argentina). S.B.D thanks the partial support from CNQq, Brazil. F.K. acknowledges the support of FAPESP (São Paulo, Brazil). The authors thank C. Bertulani for careful reading and revision of the manuscript.

References

- [1] Goriely S, Demetriou P, Janka H-Th, Pearson J M and Samyn M 2005 *Nucl. Phys. A* **758** 587
Arnould M, Goriely S and Takahashi K 2007 *Phys. Rep.* **450** 97
- [2] Hillebrandt W 2002 *Eur. Phys. Jour. A* **15** 53
- [3] Borzov I N and Goriely S 2003 *Preprint* www1.jinr.ru/Archive/Pepan/2003-v34/v-34-6/pdf_obzory/v34p6_01.pdf
- [4] Takahashi K and Yamada M 1969 *Prog. Theor. Phys.* **41** 1470
- [5] Koyama S, Takahashi K and Yamada M 1970 *Prog. Theor. Phys.* **44** 663
- [6] Kondoh T, Tachibana T and Yamada M 1985 *Prog. Theor. Phys.* **74** 708
- [7] Tachibana T, Yamada M and Yoshida Y 1990 *Prog. Theor. Phys.* **84** 641 and references therein
- [8] T. Tachibana, M. Yamada and N. Yoshida, *Prog. Theor. Phys.* **84**, 641 (1992);
- [9] Nakata H, Tachibana T and Yamada M 1997 *Nucl. Phys. A* **625** 521
- [10] Qian Y Z, Haxton W C, Langanke K, and Vogel P 1997 *Phys. Rev. C* **55** 1532
- [11] Langanke K 1999 *Phys. Rev. Lett.* **83** 4502

Eqs. (3.11) and (3.12)], instead of [9, Eq. (48)].

- Martinez-Pinedo G 2000 *Nucl. Phys. A* **668** 357c
Langanke K 2006 *Phys. Scr. T* **125** 26
- [12] Borzov I N and Goriely S 2000 *Phys. Rev. C* **62** 035501
[13] Goriely S and Khan E 2002 *Nucl. Phys. A* **706** 217
[14] Itoh N, Kohyama Y and Fujii A 1997 *Nucl. Phys. A* **287** 501; Itoh N and Kohyama Y 1997 *Nucl. Phys. A* **306** 527 15
[15] E. Feenberg and G. Trigg, *Rev. Mod. Phys.* **22** (1950) 399.
[16] Rose M E 1960 *Relativistic Electron Theory* ed John Wiley & Sons Inc. (New York) Chap. Brysk H and Rose M E 1958 *Rev. Mod. Phys.* **30** 1169
[17] Wapstra A H, Audi G and Hoekstra R 1988 *Atomic Data and Nuclear Data Tables* **39** 281
[18] Tachibana T, Uno M, Yamada M and Yamada S 1988 *Atomic Data and Nuclear Data Tables* **39** 251
[19] Krmpotić F, Samana A and Mariano A 2005 *Phys. Rev. C* **71** 044319
[20] Horen D J *et al* 1980 *Phys. Lett. B* (**95** 27
Horen D J *et al* 1981 *Phys. Lett. B* (**99** 383
Gaarde C *et al* 1981 *Nucl. Phys. A* **369** 258
[21] Nakayama K, Galeão A P and Krmpotić F 1982 *Phys. Lett. B* **114** 217
Nakayama K, Galeão A P and Krmpotić F 1983 *Nucl. Phys. A* **399** 478
[22] Bohr A and Mottelson B R 1975 *Nuclear Structure* (Benjamin, New York) Vol. 2
[23] Bender M *et al* 2002 *Phys. Rev. C* **65** 054322
[24] Langanke K and Martinez-Pinedo G 2000 *Nucl. Phys. A* **673** 481
[25] Surman R and Engel J 1998 *Phys. Rev. C* **58** 2526
[26] Kar K *et al* 1998 *J. Phys. G: Nucl. Part. Phys.* **24** 1641
[27] Sutaria F K and Ray A 1995 *Phys. Rev. C* **52** 3460
[28] Kar K and Sarkar S 1994 *Astr. Jour.* **434** 662
[29] Dean D J *et al* 1994 *Phys. Rev. Lett.* **72** 4066
[30] Kar K, Sarkar S and Ray A 1991 *Phys. Lett B* **261** 217
[31] Cooperstein J and Wambach J 1984 *Nuc. Phys. A* **420** 591
[32] Hektor A *et al* 2000 *Phys. Rev. C* **61** 055803
[33] Pritychenko B 2006 *Nuclear Wallet Cards* <http://www.nndc.bnl.gov/wallet>
[34] Samana A and Krmpotić F 2006 *Ann. of the XXVIII Workshops in Nuclear Physics in Brazil* (Livraria da Física, São Paulo) in press
[35] Keil M, Raffel G G and Hanka H-T 2003 *Astr. Jour.* **590** 971
[36] Jachowicz N and McLaughlin G C 2006 *Phys. Rev. Lett.* **96** 172301
[37] Lissia M and Quarati P 2005 *Europhysics New* **36** 211
[38] Krmpotić F, Nakayama K and Galeão A P 1983 *Nucl. Phys. A* **339** 475
[39] Moniz E J 1969 *Phys. Rev.* **184** 1154
Smith R A and Moniz E J 1972 *Nucl. Phys. B* **43** 605
[40] Kolbe E, Langanke K and Krewald S 1994 *Phys. Rev. C* **49** 1122
[41] Athanassopoulus C *et al* 1998 *Phys. Rev. C* **58** 2489
Athanassopoulus C *et al* 1998 *Phys. Rev. Lett.* **81** 1774
[42] Terasawa M, Langanke K, Kajino T and Mathews G J 2004 *Astr. Jour.* **608** 470

Table 1. Standard deviations σ_N (in units of MeV) and mismatch factors η for β^- -decay. Gaussian single-particle strength probability function $D_X(E)$ was adopted. σ_N and η (σ_N^* and η^*) indicate the results obtained with E_{GT} approximated from Eq. (13) (Eq. (11)). Parenthetically are shown the values obtained by Takahashi *et al* [4] for a different data set of nuclei. The electronic neutrino cross-section are evaluated with the underlined values of σ_N .

$N - Z$ (parent)	N_0	χ_A^2				χ_B^2			
		σ_N^*	η^*	σ_N	η	σ_N^*	η^*	σ_N	η
odd-odd	54	13.3 (5.0)	9.7 (45.5)	17.6	10.7	8.6	10.6	<u>15.8</u>	10.7
even-even	43	13.5 (4.5)	9.3 (12.9)	16.3	10.0	9.7	14.6	<u>15.8</u>	10.0
odd-even	40	13.0 (5.1)	6.1 (9.4)	16.8	6.4	4.1	15.6	<u>7.2</u>	9.8
even-odd	55	13.8 (5.1)	7.3 (6.5)	17.6	7.7	10.4	7.4	<u>16.5</u>	7.7

Table 2. Standard deviations σ_N (in units of MeV) and mismatch factors η for β^+ decay and electron-capture. Gaussian single-particle strength function D_{GT} was used. The energy E_{GT} has been evaluated from Eq. (13). The remaining notation is the same as in Table 1. No minimum has been found for the χ_A^2 -function in the case of even-even parent nuclei.

$N - Z$ (parent)	N_0	χ_A^2		χ_B^2	
		σ_N	η	σ_N	η
odd-odd	23	9.7	10.7	<u>10.4</u>	10.7
even-even	24	-	-	<u>9.9</u>	5.2
odd-even	32	12.5	6.4	<u>11.8</u>	9.8
even-odd	17	12.2	7.7	<u>12.2</u>	7.7

Table 3. Standard deviations σ_N (in units of MeV) and mismatch factors η for β^- -decay and electron-capture, obtained from the minimization of the χ_B^2 -function. Lorentzian single-particle strength probability function was used. The energy E_{GT} has been evaluated from Eq. (13).

$N - Z$	β^- decay			e^- -capture		
(parent)	N_0	$\Gamma_N/2$	η	N_0	$\Gamma_N/2$	η
odd-odd	54	15.2	12.7	23	9.8	11.3
even-even	43	15.4	11.6	24	9.4	6.5
odd-even	40	8.5	8.0	32	11.3	6.4
even-odd	55	15.7	8.6	17	11.5	8.0

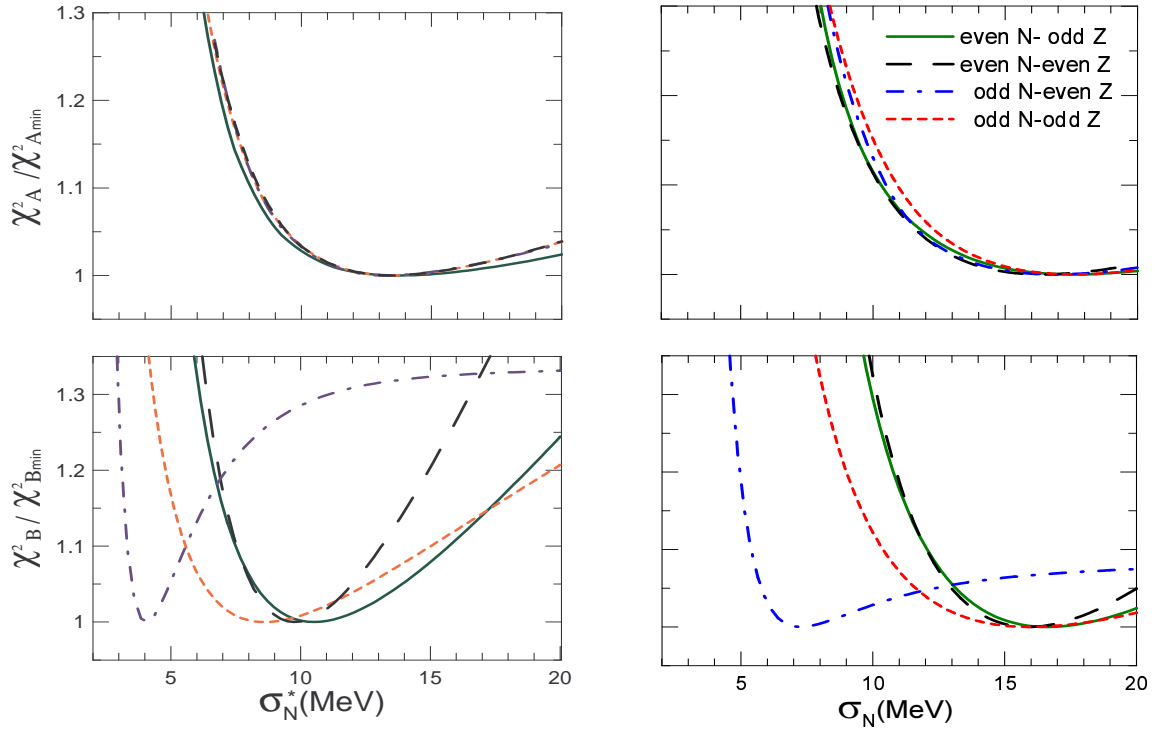


Figure 1. Comparison between χ^2 functions (normalized to the minimum) for the β^- -decay. Two types of approximations were used for the energy of the GTR: the left panel shows the results obtained with the original estimate (11); the right panel includes the energy difference between the GTR and the IAS through the Eq. (13).

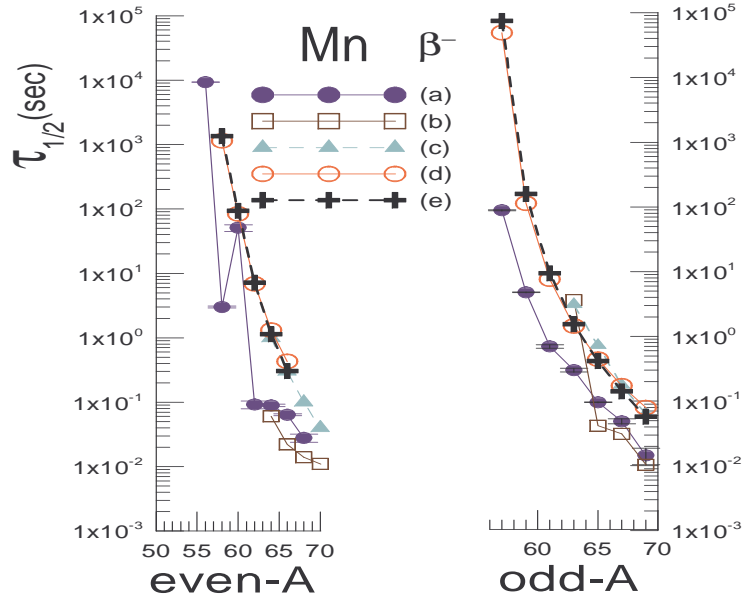


Figure 2. (Color online) Comparison of β^- -decay half-lives for Mn: (a) experimental; (b) ETFSI+CQRPA [12]; (c) ETFSI+GT2 [7]; (d) GTBD with E_{GT} from Eq. (13); and (e) GTBD with E_{GT} from Eq. (11). In both GTBD calculations the gaussian type functions for $D_{F,GT}(E)$ was used.

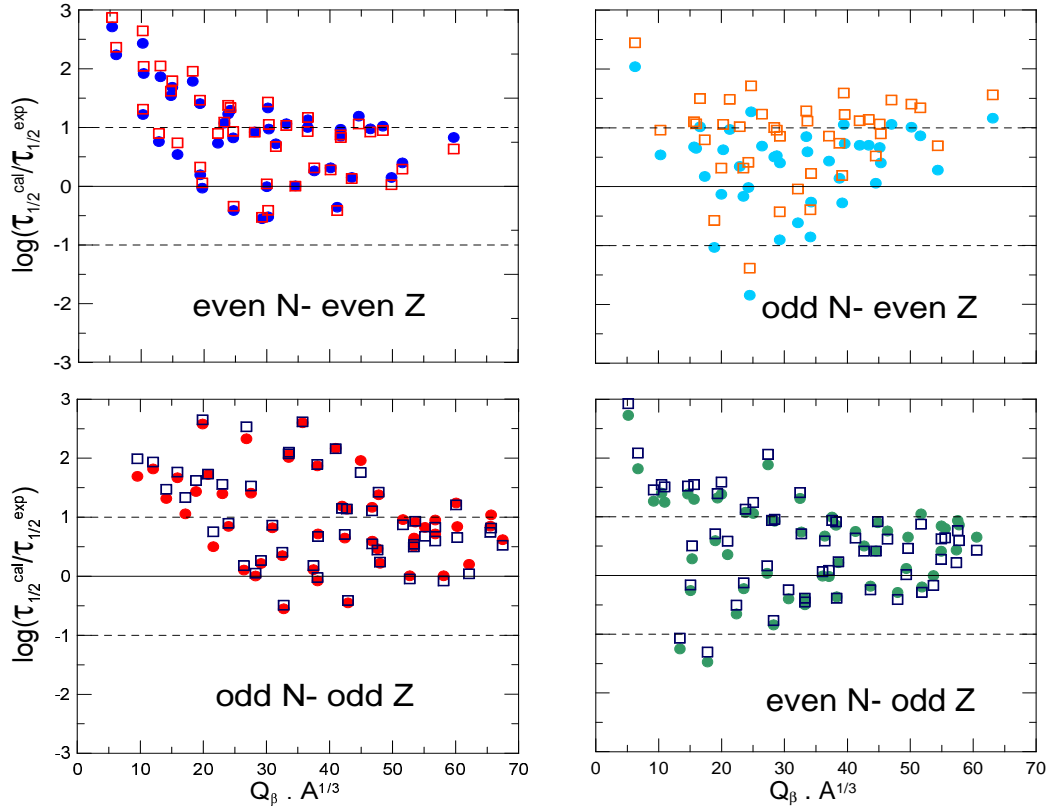


Figure 3. (Color online) $\log(\tau_{1/2}^{calc}/\tau_{1/2}^{exp})$ as a function of $Q_\beta A^{1/3}$ for β^- -decay of nuclei with $A < 70$. Gaussian functions were used for $D_X(E)$. We present the values obtained with the approximations (13) (filled circles) and (11) (hole squares) for E_{GT} .

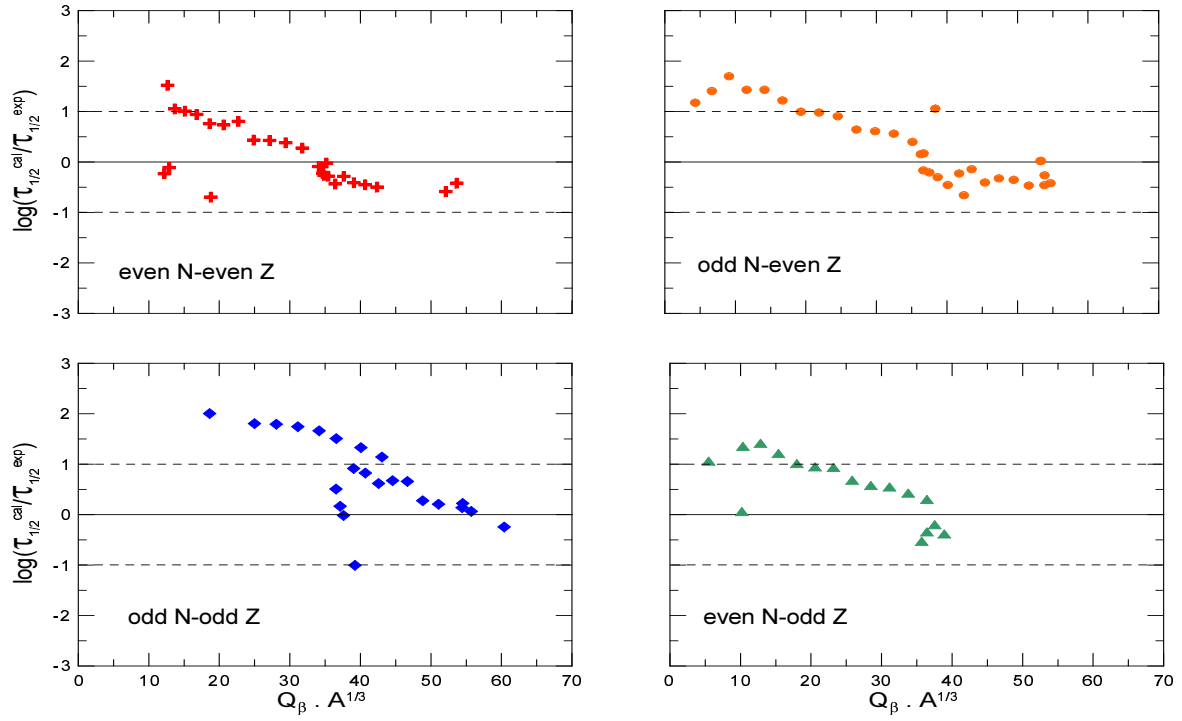


Figure 4. (Color online) $\log(\tau_{1/2}^{calc}/\tau_{1/2}^{exp})$ as a function of $QA^{1/3}$ for electron-capture of nuclei with $A < 70$. Gaussian functions were used for $D_X(E)$ and E_{GT} was calculated from Eq. (13).

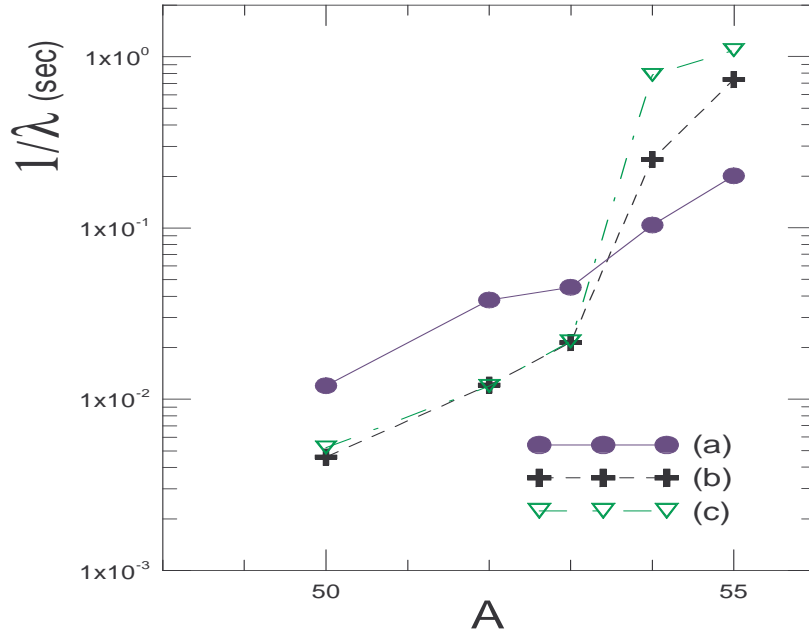


Figure 5. (Color online) Electron-capture rates for Ni isotopic chain: (a) experimental; (b) GTBD with gaussian type function; and (c) GTBD with Lorentz type function. The energy of the GTR was approximated by Eq.(13).

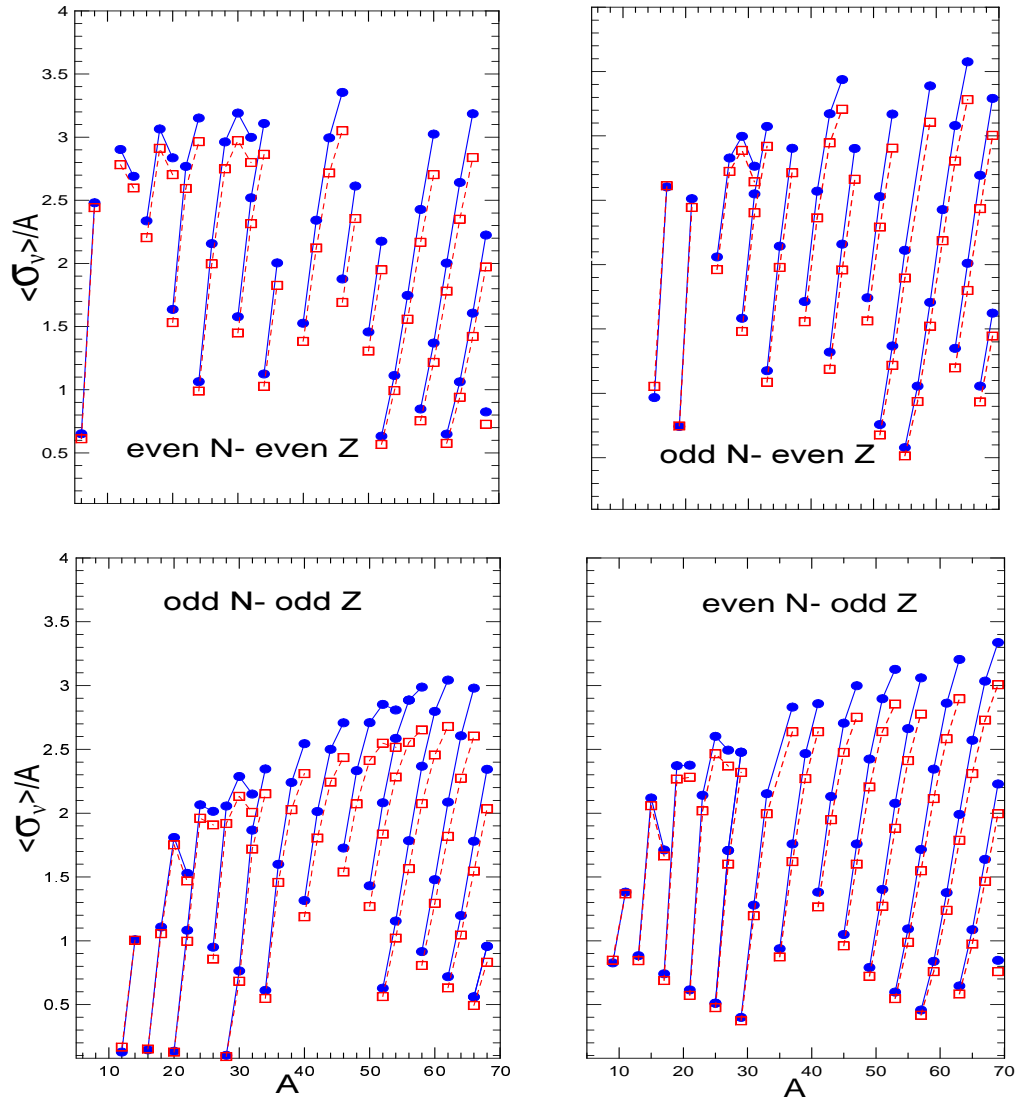


Figure 6. (Color online) Thermal reduced ν_e -nucleus cross section $\langle\sigma_\nu\rangle/A$ (in units of 10^{-40} cm^2) for β^- emitters with $A < 70$. Gaussian functions were used for $D_X(E)$. Results obtained with both approximations for the GTR are presented; with parameters values given by Eq. (11) (filled circles) and by Eq. (13) (hole squares).

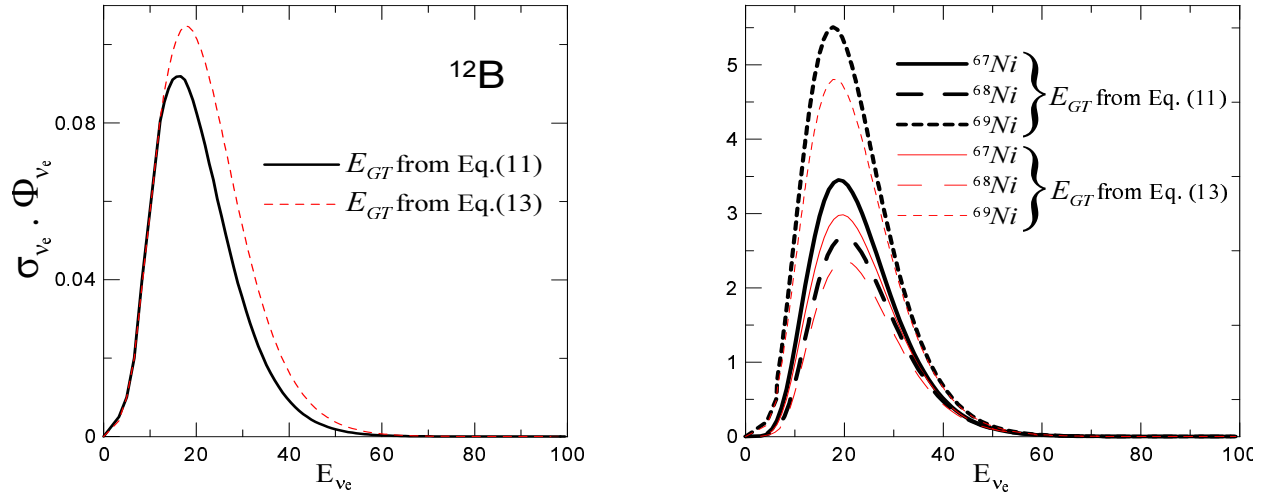


Figure 7. Results for $\sigma(E_\nu)\Phi(E_\nu)$ (in units of 10^{-42} cm^2/MeV). Gaussian functions were used for $D_X(E)$, and the results with both (11) and (13) approximations for E_{GT} are shown; for ^{12}B (left panel) and for $^{67,68,69}\text{Ni}$ isotopes (right panel).

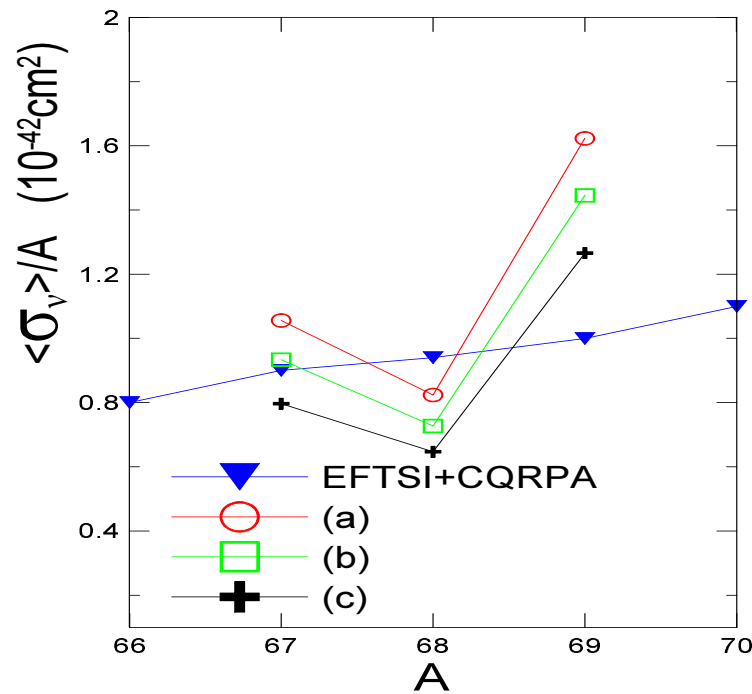


Figure 8. (Color online) Comparison between microscopic EFTSI+CQRPA calculation from Ref. [12] and our GTNC results for the electronic thermal reduced neutrino cross section (in units of 10^{-42} cm^2) for some Ni isotopes. The results obtained with gaussian strength functions are shown in (a) with E_{GT} from (11), and in (b) with E_{GT} from (13). The calculations with Lorentz distribution and E_{GT} from (13) are shown in (c).

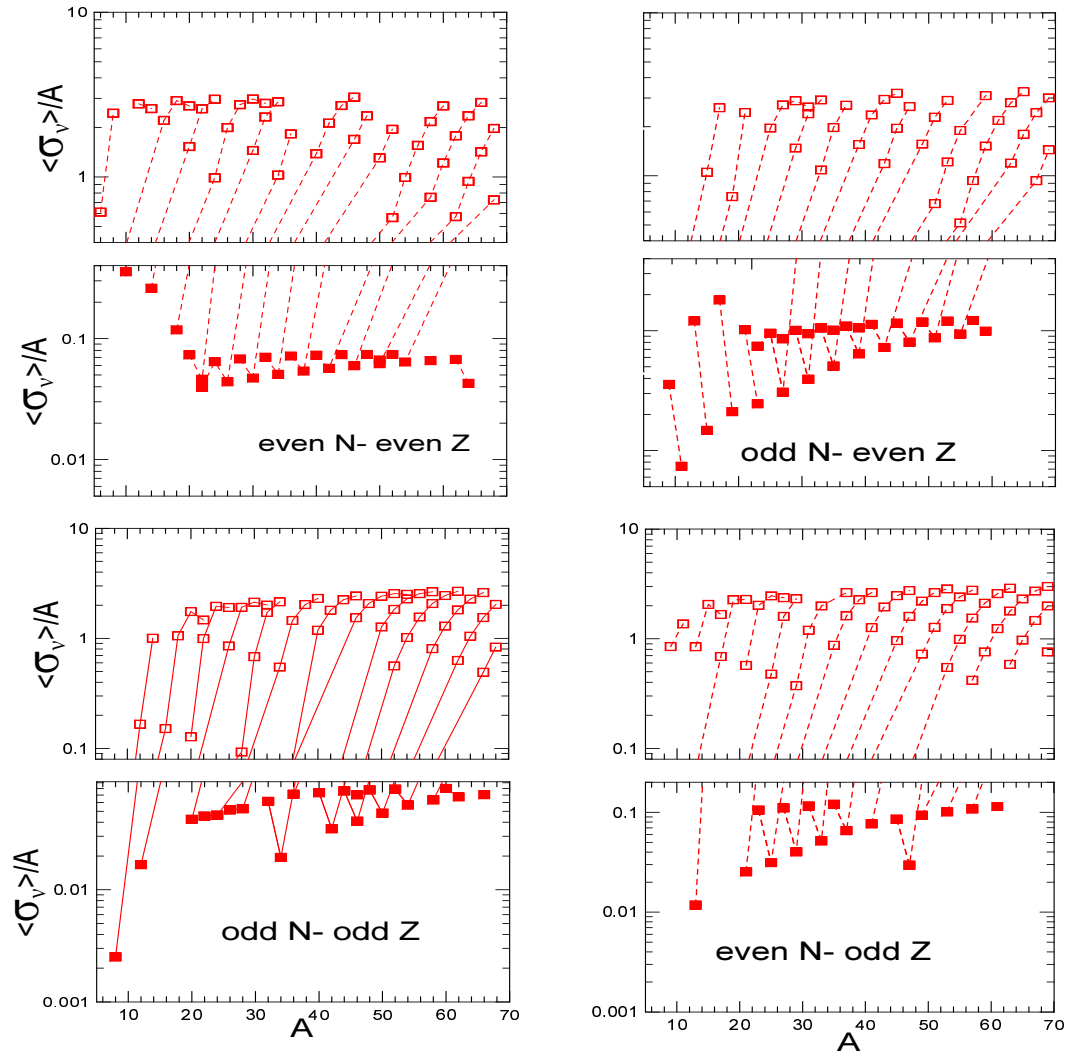


Figure 9. (Color online) Thermal reduced ν_e -nucleus cross section (in units 10^{-40} cm^2) for the $A < 70$ region with the neutrino flux at $T_\nu = 4$ MeV. The Eq. (13) for E_{GT} was used together with the gaussian strength function. We present the results for electron-capture (filled squares) and β^- emitters (hole squares).